

Changing seasonality of panarctic tundra vegetation in relationship to climatic variables

This content has been downloaded from IOPscience. Please scroll down to see the full text.

2017 Environ. Res. Lett. 12 055003

(<http://iopscience.iop.org/1748-9326/12/5/055003>)

View [the table of contents for this issue](#), or go to the [journal homepage](#) for more

Download details:

IP Address: 137.229.93.213

This content was downloaded on 08/05/2017 at 20:01

Please note that [terms and conditions apply](#).

You may also be interested in:

[Spatial and temporal patterns of greenness on the Yamal Peninsula, Russia: interactions of ecological and social factors affecting the Arctic normalized difference vegetation index](#)

D A Walker, M O Leibman, H E Epstein et al.

[Environment, vegetation and greenness \(NDVI\) along the North America and Eurasia Arctic transects](#)

D

A Walker, H E Epstein, M K Raynolds et al.

[Circumpolar Arctic vegetation: a hierarchical review and roadmap toward an internationally consistent approach to survey, archive and classify tundra plot data](#)

D A Walker, F J A Daniëls, I Alsos et al.

[Increased wetness confounds Landsat-derived NDVI trends in the central Alaska North Slope region, 1985–2011](#)

Martha K Raynolds and Donald A Walker

[Relationships between declining summer sea ice, increasing temperatures and changing vegetation in the Siberian Arctic tundra from MODIS time series \(2000–11\)](#)

L P Dutrieux, H Bartholomeus, M Herold et al.

[Land cover and land use changes in the oil and gas regions of Northwestern Siberia under changing climatic conditions](#)

Qin Yu, Howard E Epstein, Ryan Engstrom et al.

[Recent changes in phenology over the northern high latitudes detected from multi-satellite data](#)

Heqing Zeng, Gensuo Jia and Howard Epstein

Environmental Research Letters



LETTER

Changing seasonality of panarctic tundra vegetation in relationship to climatic variables

OPEN ACCESS

RECEIVED

6 December 2016

REVISED

17 March 2017

ACCEPTED FOR PUBLICATION

4 April 2017

PUBLISHED

5 May 2017

Original content from this work may be used under the terms of the [Creative Commons Attribution 3.0 licence](#).

Any further distribution of this work must maintain attribution to the author(s) and the title of the work, journal citation and DOI.



Uma S Bhatt^{1,8}, Donald A Walker², Martha K Reynolds², Peter A Bieniek³, Howard E Epstein⁴, Josefino C Comiso⁵, Jorge E Pinzon⁶, Compton J Tucker⁶, Michael Steele⁷, Wendy Ermold⁷ and Jinlun Zhang⁷

¹ Department of Atmospheric Sciences in the College of Natural Science and Mathematics, Geophysical Institute, University of Alaska Fairbanks, 903 Koyukuk Dr., Fairbanks, AK 99775-7320, United States of America

² Department of Biology and Wildlife in the College of Natural Science and Mathematics, Institute of Arctic Biology, University of Alaska, Fairbanks, AK 99775-7000, United States of America

³ International Arctic Research Center, University of Alaska, Fairbanks, AK 99775-7340, United States of America

⁴ Department of Environmental Sciences, University of Virginia, 291 McCormick Rd, Charlottesville, VA 22904-4123, United States of America

⁵ Cryospheric Sciences Branch, NASA, NASA Goddard Space Flight Center, Code 614.1, Greenbelt, MD 20771, United States of America

⁶ Biospheric Science Branch, NASA, NASA Goddard Space Flight Center, Code 614.1, Greenbelt, MD 20771, United States of America

⁷ Applied Physics Laboratory, University of Washington, 1013 NE 40th Street, Seattle, WA 98105, United States of America

⁸ Author to whom any correspondence should be addressed.

E-mail: usbhatt@alaska.edu

Keywords: tundra vegetation greening and browning, Arctic climate variability, sea ice, seasonality, NDVI

Abstract

Potential climate drivers of Arctic tundra vegetation productivity are investigated to understand recent greening and browning trends documented by maximum normalized difference vegetation index (NDVI) (MaxNDVI) and time-integrated NDVI (TI-NDVI) for 1982–2015. Over this period, summer sea ice has continued to decline while oceanic heat content has increased. The increases in summer warmth index (SWI) and NDVI have not been uniform over the satellite record. SWI increased from 1982 to the mid-1990s and remained relatively flat from 1998 onwards until a recent upturn. While MaxNDVI displays positive trends from 1982–2015, TI-NDVI increased from 1982 until 2001 and has declined since. The data for the first and second halves of the record were analyzed and compared spatially for changing trends with a focus on the growing season. Negative trends for MaxNDVI and TI-NDVI were more common during 1999–2015 compared to 1982–1998.

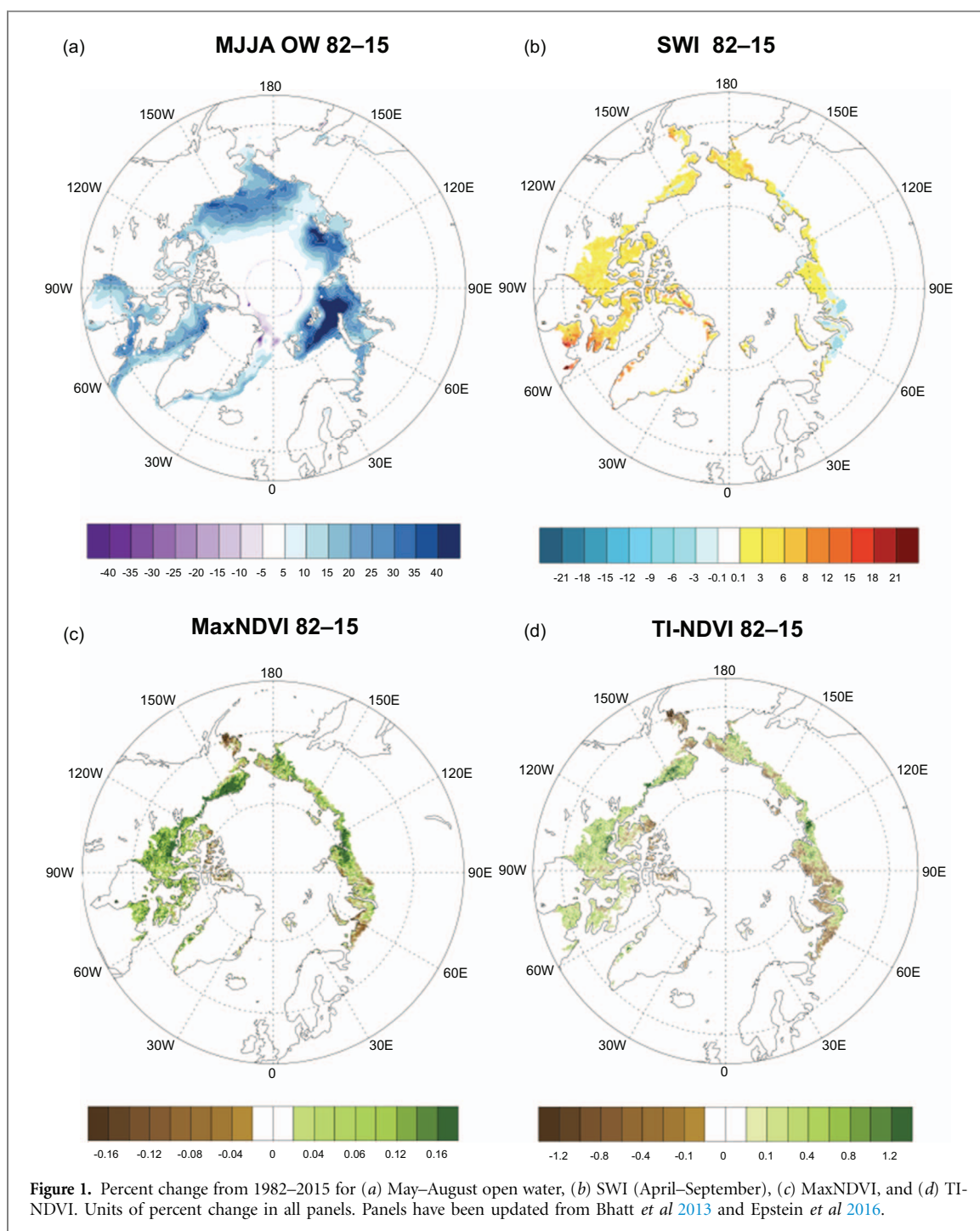
Trend analysis within the growing season reveals that sea ice decline was larger in spring for the 1982–1998 period compared to 1999–2015, while fall sea ice decline was larger in the later period. Land surface temperature trends for the 1982–1998 growing season are positive and for 1999–2015 are positive in May–June but weakly negative in July–August. Spring biweekly NDVI trends are positive and significant for 1982–1998, consistent with increasing open water and increased available warmth in spring. MaxNDVI trends for 1999–2015 display significant negative trends in May and the first half of June.

Numerous possible drivers of early growing season NDVI decline coincident with warming temperatures are discussed, including increased standing water, delayed spring snow-melt, winter thaw events, and early snow melt followed by freezing temperatures. Further research is needed to robustly identify drivers of the spring NDVI decline.

1. Introduction

Three decades of remotely sensed normalized difference vegetation index (NDVI) data document an

overall increase in Arctic tundra vegetation greenness (Myneni *et al* 1997, Jia *et al* 2003, Walker *et al* 2009, Xu *et al* 2013, Ju and Masek 2016) but the trends display considerable spatial variability. NDVI represents



vegetation productivity as measured by aboveground biomass (Tucker and Sellers 1986, Shippert *et al* 1995, Stow *et al* 2004) and has a strong relationship with biomass throughout the panarctic tundra (Epstein *et al* 2012). Panarctic tundra vegetation greening is associated with increases in summer warmth (Jia *et al* 2003, Hope *et al* 2005) that are, in large-part, driven by summer sea ice retreat along Arctic coasts (Bekryaev *et al* 2010, Bhatt *et al* 2010, Dutrieux *et al* 2012). Climate variability over the Arctic Ocean plays an important role in tundra vegetation productivity because so much of the Arctic tundra biome is located near Arctic Ocean coastlines (Walker *et al* 2005).

Trends covering the period 1982–2015 are overall positive for summer open water, summer warmth index (SWI, the sum of the monthly mean temperatures above 0°C from April to September), MaxNDVI (peak NDVI) and time-integrated NDVI (TI-NDVI, sum of biweekly NDVI values above 0.05 from May–September) (figure 1). Increased open water during summer (figure 1(a)) resulting from sea ice retreat along the Arctic coast is consistent with warming land surface temperatures (figure 1(b)) and increased vegetation greenness (figure 1(c) and (d)). A more detailed examination shows that not all regions have positive trends, for example, there is an area of cooling in western Eurasia, which is broadly co-located

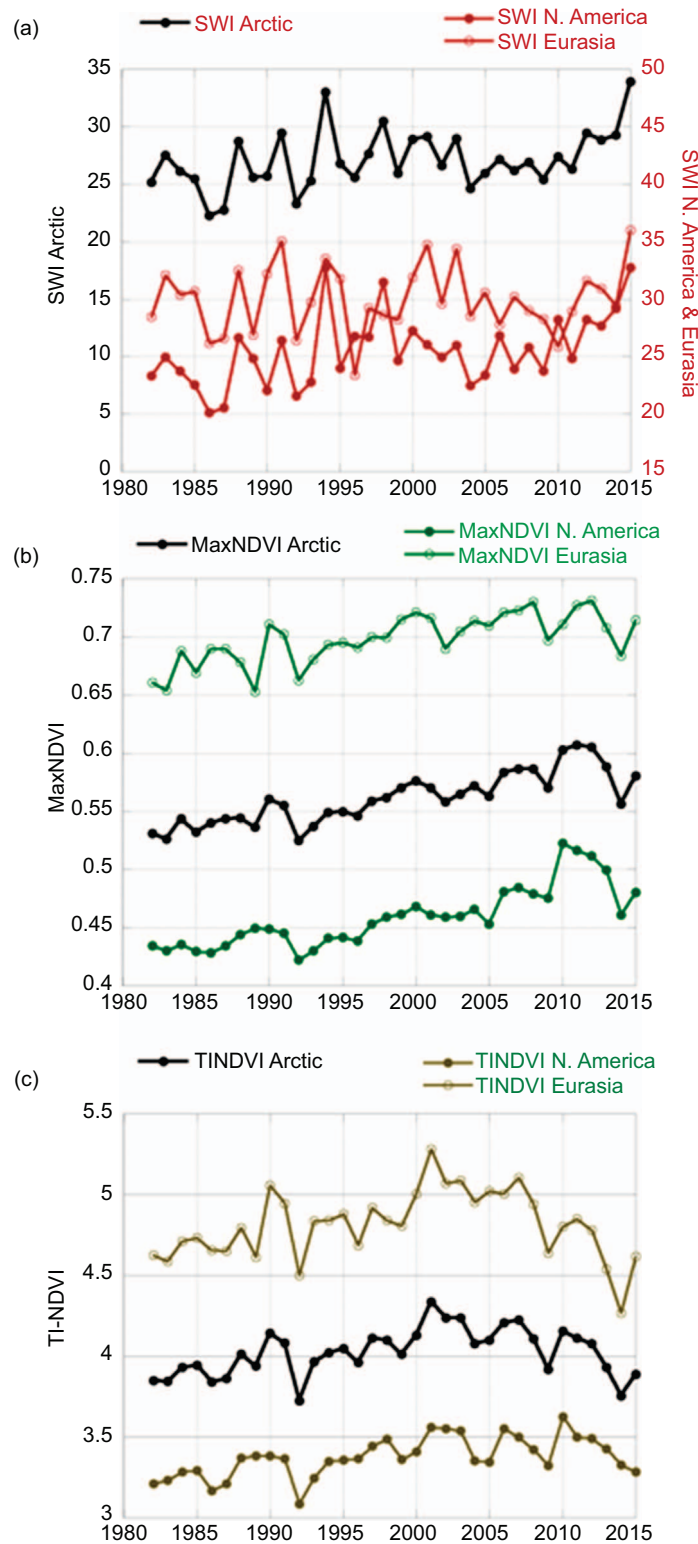


Figure 2. Time series of (a) SWI ($^{\circ}\text{C month}$), (b) MaxNDVI (unitless), and (c) TI-NDVI (unitless) for each growing season from 1982–2015. Each panel displays time series for the Arctic, Eurasia, and North America. Note that there is a different scale for the two y -axes in panel (a) where Arctic is given on the left axis while Eurasia and North America are represented on the right axis.

with maxNDVI and TI-NDVI declines (figure 1). While sea ice decline has continued over the satellite record, summer land surface temperatures and vegetation productivity measures have not continued to simply increase (Epstein *et al* 2015) (figure 2). Time series of SWI for the panarctic, North American Arctic and Eurasian Arctic reveal large interannual variability

and low-frequency variability that is offset between North America and Eurasia (figure 2(a)). The Eurasian SWI decreased from 2004–2010, while in North America SWI declined from 1998–2005, but both show SWI increases since 2010 (figure 2(a)). The MaxNDVI time series shows a steady increase over the record (figure 2(b)) while TI-NDVI trends (figure 2

(c) have flattened or even declined (e.g. Eurasia) over the last decade (Bhatt *et al* 2013). This suggests that likely multiple processes influence vegetation productivity beyond secular greening associated with increased summer warmth.

Tundra vegetation productivity is primarily controlled by temperature (Bliss 1997, Chernov and Matveyeva 1997, Callaghan *et al* 2004) where increased warmth leads to increased biomass. The heterogeneity in recent trends suggests a closer examination of moisture, which also plays a role in plant productivity. Ground-based observations along the North American (NAAT) and Eurasian (EAT) Arctic Transects (Walker *et al* 2012b) highlight differences in vegetation due to temperature, moisture and substrate factors. The NAAT and EAT have similar temperature regimes and plant distributions for a given bioclimate subzone (Walker *et al* 2005) but the EAT receives more annual precipitation and has more moss biomass in subzones B-E (Walker *et al* 2012b). Climate research based on global modeling consistently shows that as the climate warms the total snowfall decreases but it increases at higher latitudes and altitudes where below-freezing temperatures prevail in winter (Krasting *et al* 2013, Kapnick and Delworth 2013).

Increasing snow at high latitudes has not yet been clearly documented in contemporary observations for the panarctic but several recent observationally-based studies show increases in snow amounts in Eurasia (Bulygina *et al* 2009, Cohen *et al* 2012), Abisko Sweden (Kohler *et al* 2006), and northern Alaska (Urban and Clow 2014, Clow 2014, Cherry *et al* 2014, Vikhamar-Schuler *et al* 2010). Increased transport of moist static energy in a CO₂ enhanced climate is a primary mechanism by which the Arctic atmospheric column warming is amplified (Alexeev *et al* 2005). Zhang *et al* (2012) found that moisture transport into Eurasia increased during winter in the NCEP/NCAR Reanalysis, which is consistent with increased snow amounts. An analysis of remote sensing data sets from 2000–2010 found that a sea ice concentration decline of 1% leads to a 0.36%–0.47% increase in cloud cover (Liu *et al* 2012). Some of this moisture is expected to result in increased precipitation as shown in an investigation of deuterium excess measurements where sea ice decline coincides with an increase in high-latitude precipitation originating in the Arctic (Kopeck *et al* 2016). Reduced sea ice imposed in a regional model in the Beaufort Sea leads to increased precipitable water indicating that increased moisture is available in the atmospheric column to form clouds and precipitation (Bieniek *et al* 2015). Therefore, once climate warming has melted a sufficient amount of sea ice, hydro-climate processes likely play a larger role as drivers of vegetation productivity than when the ice first began to decline and contributed to large local land surface warming.

The new contribution of this study is to document panarctic trends within a season over the period

1982–2015 for the GIMMS NDVI3g for Arctic tundra together with landsurface temperatures, sea ice concentration, and ocean-heat content. We focused particularly on seasonality of trends to investigate the times of year that are changing the most, and relating these to interactions between the vegetation and associated climate drivers. Recent work shows that the warming and greening trends over panarctic tundra have slowed down (Walker *et al* 2012a, Bhatt *et al* 2013, Epstein *et al* 2015) and are more heterogeneous. This study compares the seasonality and trends during 1982–1998 with those from 1999–2015. These periods were chosen by determining the timing of trend change (1998 \pm 7 yr) in the panarctic SWI time series based on a parametric, nonlinear regression technique called ‘breakfit regression’ (Mudelsee 2010 2009). Exact break points vary considerably over Arctic tundra domain (Bhatt *et al* 2013), however, 1998 shows up as a global temperature peak due to the strong El Niño, is midway through the data record, and is consistent with the timing of the global ‘climate hiatus’ (Easterling and Wehner 2009). Based on this reasoning, the analysis is split into two periods as follows: 1982–1998 and 1999–2015 to investigate variations in NDVI and its climate drivers.

2. Data and methods

2.1. Data

Special Sensor Microwave Imager (SSM/I) sea ice concentrations (Comiso and Nishio 2008) and Advanced Very High Resolution Radiometer (AVHRR) radiometric surface temperature are investigated over the 1982–2015 period. The term sea ice concentration is used in this publication to describe sea ice area in units of percentage area covered. The portion of a pixel that is not covered by sea ice is denoted as open water (i.e. 100% – sea ice concentration). Summer open water (OW) is constructed by summing up the weekly May through August open-water percentage (units are % open water area within a pixel) and then dividing by the number of weeks to produce an average weekly OW amount for the summer.

The remotely-sensed surface temperature data have been corrected through effective cloud-masking techniques and calibration through the utilization of in-situ surface temperature data. Surface temperatures from the surface heat budget in the Arctic (SHEBA) experiment conducted in the central Arctic from October 1997 through September 1998 and 2 m air temperatures from meteorological stations were used to calibrate the AVHRR data. Details of this procedure can be found in Comiso (2003). SWI was calculated as the sum of average April to September monthly surface temperatures above freezing at each pixel and is in units of °C months. Note that SWI calculated using ground surface temperatures is warmer than

SWI calculated using 2 m air temperature (Raynolds *et al* 2008).

Remotely-sensed NASA GIMMS (Global Inventory Modeling and Mapping Studies) bi-weekly maximum NDVI data (Pinzon and Tucker 2014) from 1982–2015 are derived from AVHRR sensors on NOAA-7 through NOAA-18 satellites. The NDVI3g product corrected discontinuities in the GIMMS NDVI north of 72°N and permitted the first comprehensive analysis of NDVI trends in the High Arctic (Bhatt *et al* 2010). Details about the calibration process are available in Pinzon and Tucker (2014). This study used approximately 12 km resolution NDVI data to more closely match the grids used for sea ice and surface temperature. The maximum NDVI (MaxNDVI) is the highest summer NDVI value, representing peak vegetation photosynthetic capacity, and serves as an indicator of tundra biomass (Shippert *et al* 1995, Walker *et al* 2003a). The time-integrated NDVI (TI-NDVI) is the sum from May to September of biweekly values above a threshold value of 0.05, low enough to capture the often abrupt snowmelt. TI-NDVI incorporates the length of the growing season and phenological variations, better represents gross primary production than MaxNDVI (Tucker and Sellers 1986) and is better correlated with climate parameters (Bhatt *et al* 2010).

The Panarctic Ice Ocean Modeling and Assimilation System (PIOMAS) dataset (Zhang and Rothrock 2003, Steele *et al* 2011) provides biweekly ocean heat content data for 1988–2013, where sea surface temperature and sea ice concentration were assimilated into the model simulation. The heat content was calculated by vertically integrating the density of the ocean times the specific heat capacity times the ocean potential temperature minus a reference temperature of -2 °C from the surface to 100 m depth (or less depending on depth of ocean). The data were then area-averaged within a 100 km buffer of the coast of each tundra region.

The NCEP/NCAR reanalysis (Kistler *et al* 2001) provided sea level pressure (reanalysis) and the ERA-Interim (Dee *et al* 2011) 2 m air temperature for this study. Reanalyses are constructed by ingesting a variety of observations (i.e. meteorological station data, atmospheric soundings, sea surface temperature, satellite observations) into a weather forecast model to fill in data sparse regions and create a gridded 'observational' data set. These data sets have been invaluable for investigating climate variability processes over the past several decades.

2.2. Analysis methods

The scale of interest in the study is the Arctic non-alpine tundra and its continental divisions of North America and Eurasia. The analysis employs time series averaged over oceanic regions within 100 km of the Arctic coastline and over the full tundra domains at elevations < 300 m. The least-squares-fit method was

used to determine the trends of open water, SWI, MaxNDVI, and TI-NDVI in the spatial presentation (figure 1). Spatial trends are shown as a magnitude change for Open Water, SWI, TI-NDVI, and MaxNDVI over the 34 years period and are based on the pixel size of the given data set. The statistical significance of correlations and trends was assessed using the two-tailed Student's *t*-test at the 95% or greater level. Climate data variability in the Arctic displays large-amplitude multi-decadal variability along with trends (Polyakov *et al* 2013) which reduces the degrees of freedom due to large autocorrelations from year-to-year. For significance testing the reduced degrees of freedom were calculated using a lag-1 autocorrelation method outlined by Santer *et al* (2000).

3. Results

3.1. Spatial trends

SWI trends vary regionally from 1982–1998 (figure 3 (a)) with a strong warming trend over North America, particularly northern Canada, in the region between 90 and 120 °W, and a distinct cooling trend in West Siberia between 50 and 120 °E. The trend is more mixed from 1999–2015 (figure 3(b)). Trend magnitudes for SWI from 1982–1998 (first period) show increased warmth over most of the Arctic except western Eurasia, where the trends are negative (figure 3 (a)). SWI for 1999–2015 (second period) displays patches of negative trends throughout Eurasia and Alaska while the Canadian High Arctic and Greenland show mainly warming trends (figure 3(b)). The overall weakening of SWI trends since 1999 suggests that additional processes are currently operating in the Arctic tundra.

SWI trends based on 2 m air temperature from the European Center Reanalysis (ERA-Interim) for 1982–1998 (figure 3(c)) compare favorably with AVHRR based land surface temperature trends (figure 3(a)). In contrast, SWI trends from 1999–2015 based on the ERA-Interim show general warming over the tundra region (figure 3(d)) while AVHRR-based SWI shows areas of negative trends in Eurasia (figure 3(b)) suggesting that land surface and air temperature trends are diverging in recent years. Time series of SWI based on land surface and 2 m air temperature is shown in figure 4 for North America (figure 4(a)) and Eurasia (figure 4(b)). As expected, the air temperature based SWI is cooler on average than the land surface based SWI but displays similar interannual variability (correlation is about 0.6 for both regions). The trends have a similar slope in North America but are quite different in Eurasia where the air temperature based SWI is warming faster than land surface temperature based SWI (figure 4(b)). One possible local explanation for these diverging trends is the idea that a denser plant canopy with a thicker organic layer will reduce

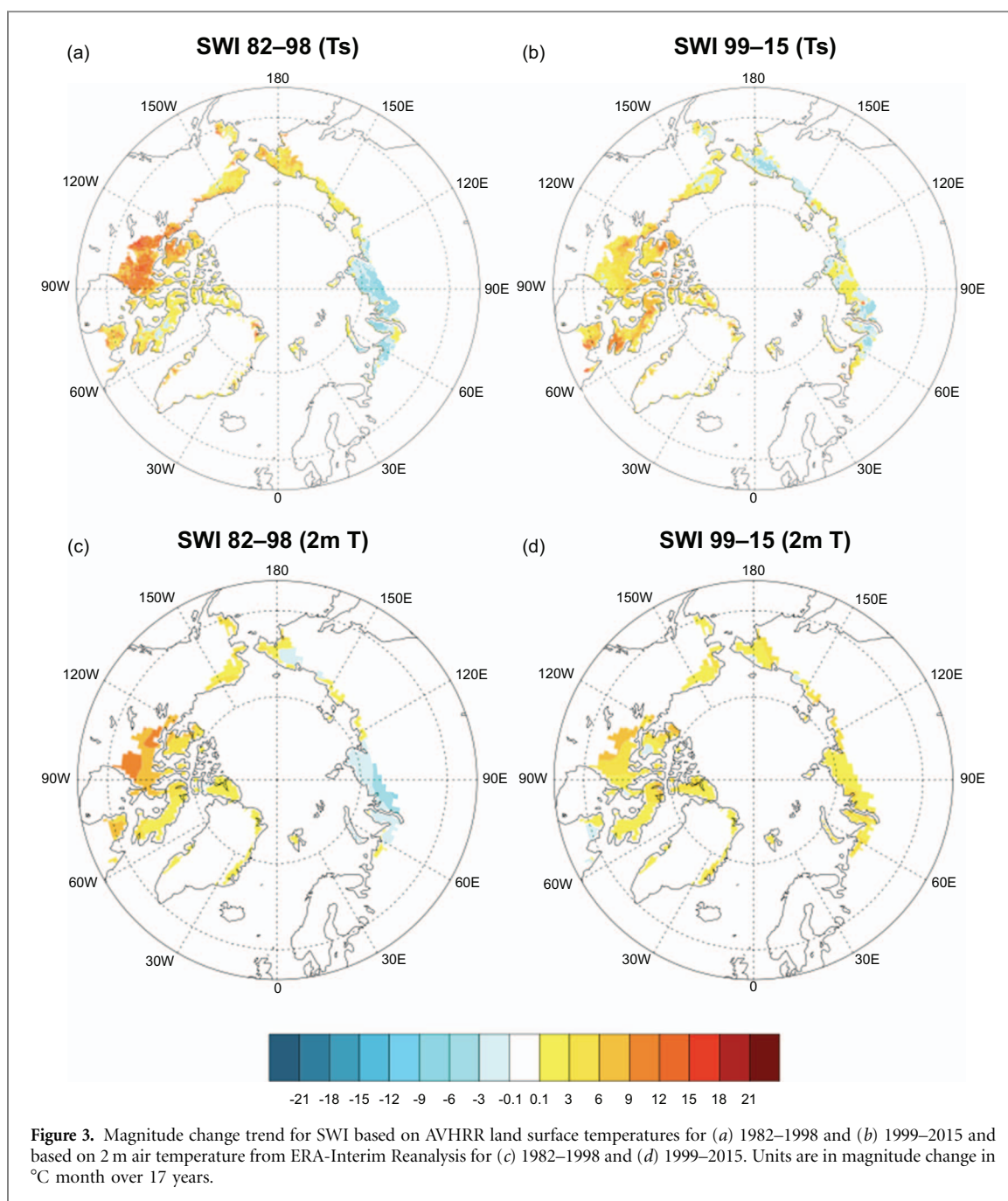
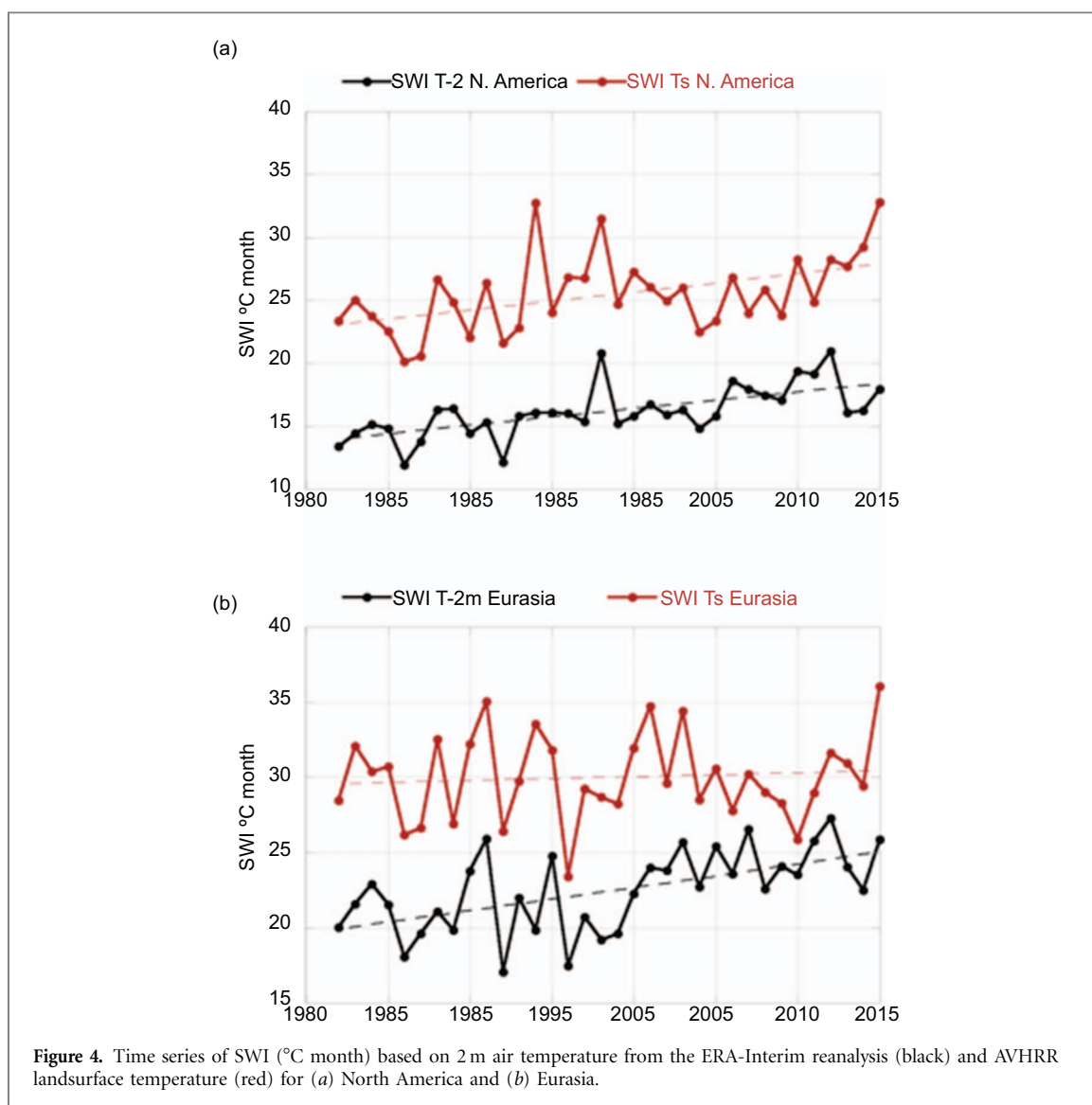


Figure 3. Magnitude change trend for SWI based on AVHRR land surface temperatures for (a) 1982–1998 and (b) 1999–2015 and based on 2 m air temperature from ERA-Interim Reanalysis for (c) 1982–1998 and (d) 1999–2015. Units are in magnitude change in °C month over 17 years.

the warming of the soil (Walker *et al* 2003b). This idea is supported by Circumpolar Active Layer Monitoring (CALM) network observations which show that from 1996–2013 the summer N-factors (ratio of ground surface to air temperatures) in bioclimate subzones C, D, and E have been decreasing (Shiklomanov and Streletskiy 2015). This is likely to be one of multiple processes operating that prevents simple interpretations of the long-term observational data. Finally, it is plausible that this discrepancy could be an artifact of the data, caused either by changes over time in the number and location of data sources for the ERA-interim data, or issues with calibrating a long-term satellite record (Urban *et al* 2013).

Overall, the panarctic tundra maxNDVI trends display more pixels with negative trends in the recent

period compared to the earlier period (figure 5). For MaxNDVI, trends for 1982–1998 (figure 5(a)) are positive (> 0.02) for 54% of the pixels and negative (< -0.02) for 6% of the pixels. Considering only pixels with significant ($p < 0.05$) trends, 14% are positive for 1982–1998. For the 1999–2015 period (figure 5(b)) trends are positive for 55% of the pixels and negative for 29% of the pixels. Significant trends are positive in 31% and negative in 14% of the pixels for 1999–2015. MaxNDVI declines are limited to the southern edges of the tundra during the period from 1982–1998 (figure 5(a)) but are found in western Eurasia, southwest Alaska, and the northern Canada in the period from 1999–2015. The positive MaxNDVI trends have become stronger in the 1999–2015 period compared to the earlier period.



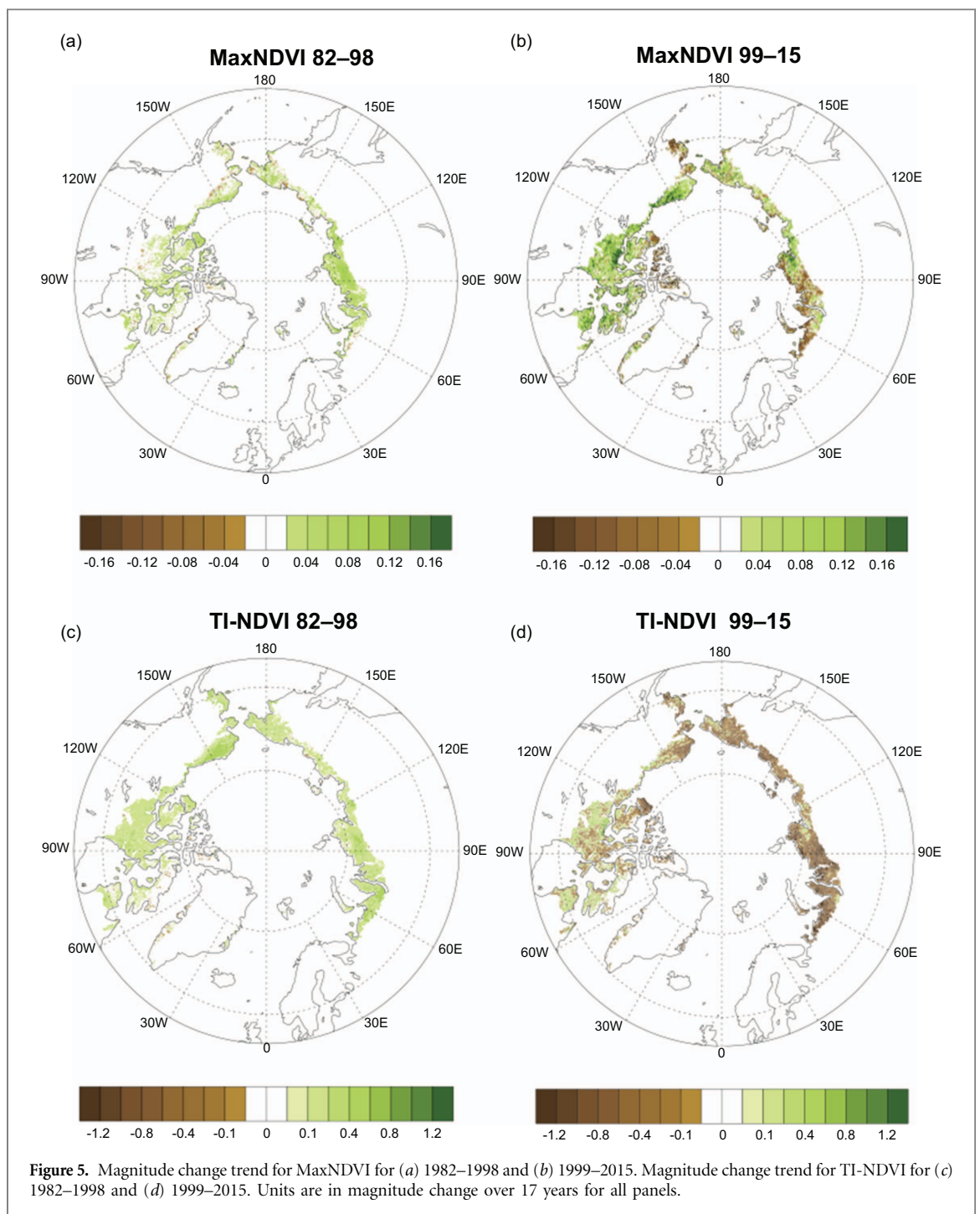
TI-NDVI magnitude trends are generally positive from 1982–1998 and largely negative for the 1999–2015 period with consistent negative trends in Eurasia in agreement with figure 2(c). Over the period 1982–1998 (figure 5(c)), 81% of the pixels have positive trends (> 0.05) and 5% have negative trends (< -0.05). Considering only pixels with significant ($p < 0.05$) trends, 17% are positive for 1982–1998. From 1999–2015 (figure 5(d)), 25% of the pixels have a positive trend while 67% have a negative trend. Significant trends for 1999–2015 are positive in 7% and negative in 34% of the pixels. Variations within a season are discussed next to understand the timing of TI-NDVI declines and possible climate drivers of these declines.

3.2. Changing seasonality

Sea ice concentration in the 100 km Arctic coastal zone has decreased more than 10% from climatology (1982–2015) between late May and November (figure 6(a)). Figure 6 displays weekly sea ice concentration climatology (blue bars) and trends (grey bars) for the full period 1982–2015 (figure 6(a)), the early period of

1982–1998 (figure 6(b)) and the recent period from 1999–2015 (figure 6(c)). From 1982–1998, the sea ice declines were larger ($> 10\%$ per 17 years) during spring and smaller in fall. Negative trends were larger ($> 10\%$ per 17 years) during fall for 1999–2015 than for 1982–1998. This analysis shows that over the satellite record, the sea ice concentration decreased first in spring followed by large declines in the fall. This is consistent with warmer atmospheric temperatures driving earlier spring breakup followed by an extended open-water season, increased heat storage in the ocean and a delayed freeze up in the fall.

Oceanic heat content in the 100 km coastal zone has increased in the Arctic (figure 7(a)) throughout the year and peak positive trends occur in late September over the 1988–2013 period. Figure 7 displays biweekly oceanic heat content climatology (orange bars) and trend (grey bars) for the period 1988–2013 in the Arctic (figure 7(a)), North America (figure 7(b)) and Eurasia (figure 7(c)). The heat content reaches its annual maximum value in early September for North American and Eurasia but the peak positive trends are in late August in North



America and in late September in Eurasia. The seasonal cycle of Eurasian fall sea ice freezeup is later than in North America and the sea ice decline is larger in fall (not shown). This is consistent with the later oceanic heat-content trend peak in Eurasia compared to North America. The ice-reduced warm ocean is a source of heat and moisture for the Arctic atmosphere in the autumn. Sea ice reduction is considered to be the underlying cause of near-surface Arctic atmospheric warming during fall (Screen and Simmonds 2010) and heat provided by the ocean further supports this idea. The positive trends in heat content are late in the growing season and could potentially impact vegetation productivity the following year by hasten-

ing spring sea ice melt. September ocean heat content in the 100 km coastal zone is correlated with sea ice concentration the following spring at -0.56 (same season correlation is -0.78), suggesting that there is memory in the system that may provide a possible link between the coastal ocean and terrestrial regions.

Summer low elevation (< 300 m) tundra land surface temperature increases have slowed down in recent years (figure 8). Figure 8 displays land surface temperature climatology (red bars) and trends (grey bars) for the full period 1982–2015 (figure 8(a)), the early period of 1982–1998 (figure 8(b)) and the recent period from 1999–2015 (figure 8(c)). From 1982–1998, there was strong warming in late winter–early

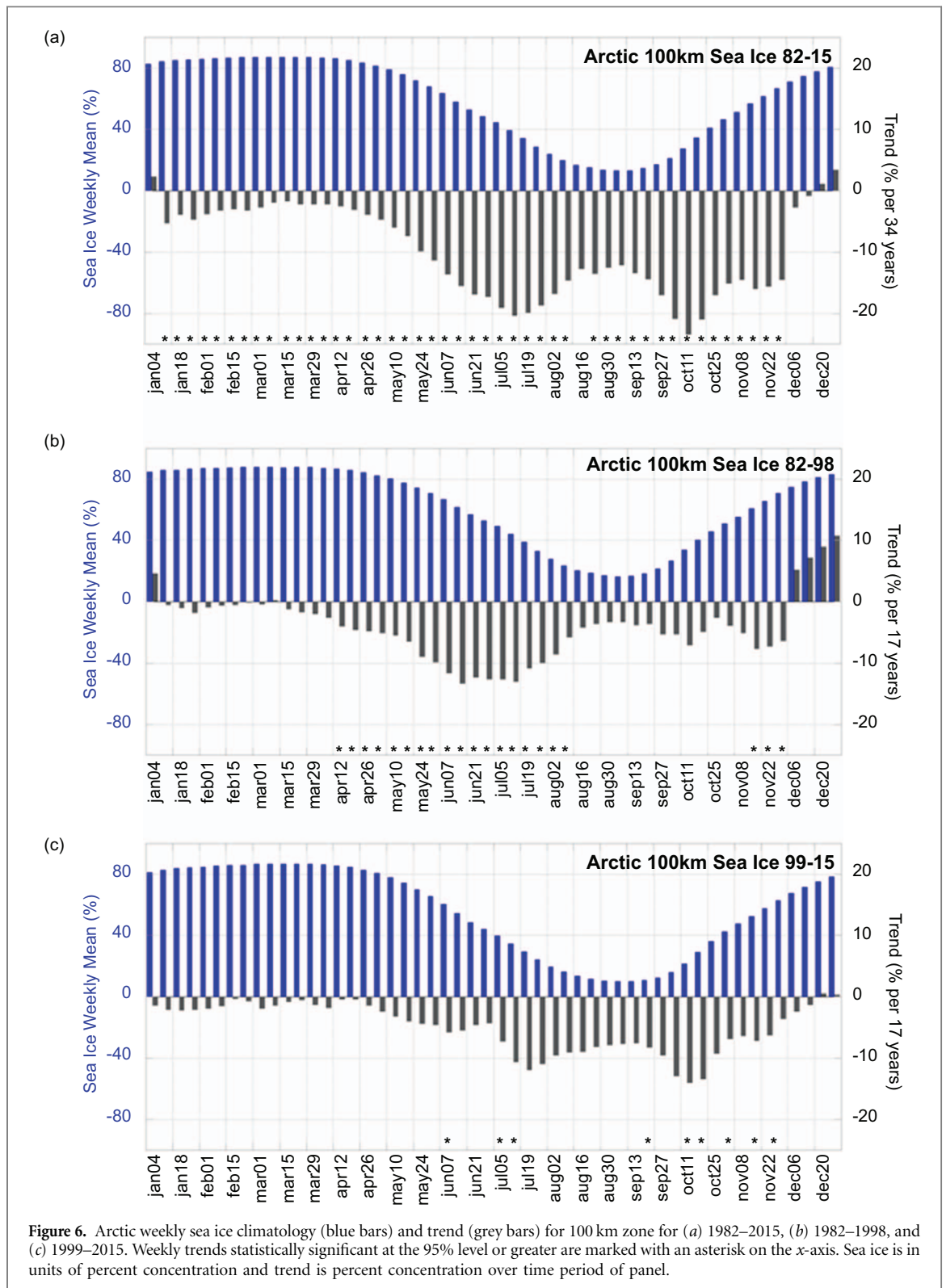


Figure 6. Arctic weekly sea ice climatology (blue bars) and trend (grey bars) for 100 km zone for (a) 1982–2015, (b) 1982–1998, and (c) 1999–2015. Weekly trends statistically significant at the 95% level or greater are marked with an asterisk on the x-axis. Sea ice is in units of percent concentration and trend is percent concentration over time period of panel.

summer (Mar–mid June) and in Oct–Nov. The late winter trends switched to strong negative values over the period 1999–2015. During 1982–1998, land surface temperatures display generally positive trends throughout the year with positive trends in May and November (figure 8(b)). Trends from 1999–2015 display modest positive values in May and June and weak negative trends from mid-July to the end of summer (figure 8(c)). These panarctic summer

cooling trends are evident in individual panarctic tundra regions except those around Greenland (Bhatt *et al* 2013). The recent declines in land surface temperature may reflect local processes, as was shown in the idealized model study by Bieniek *et al* 2015, but likely primarily result from the global climate hiatus that coincides with the 1999–2015 period and is not expected to continue much longer (Roberts *et al* 2015).

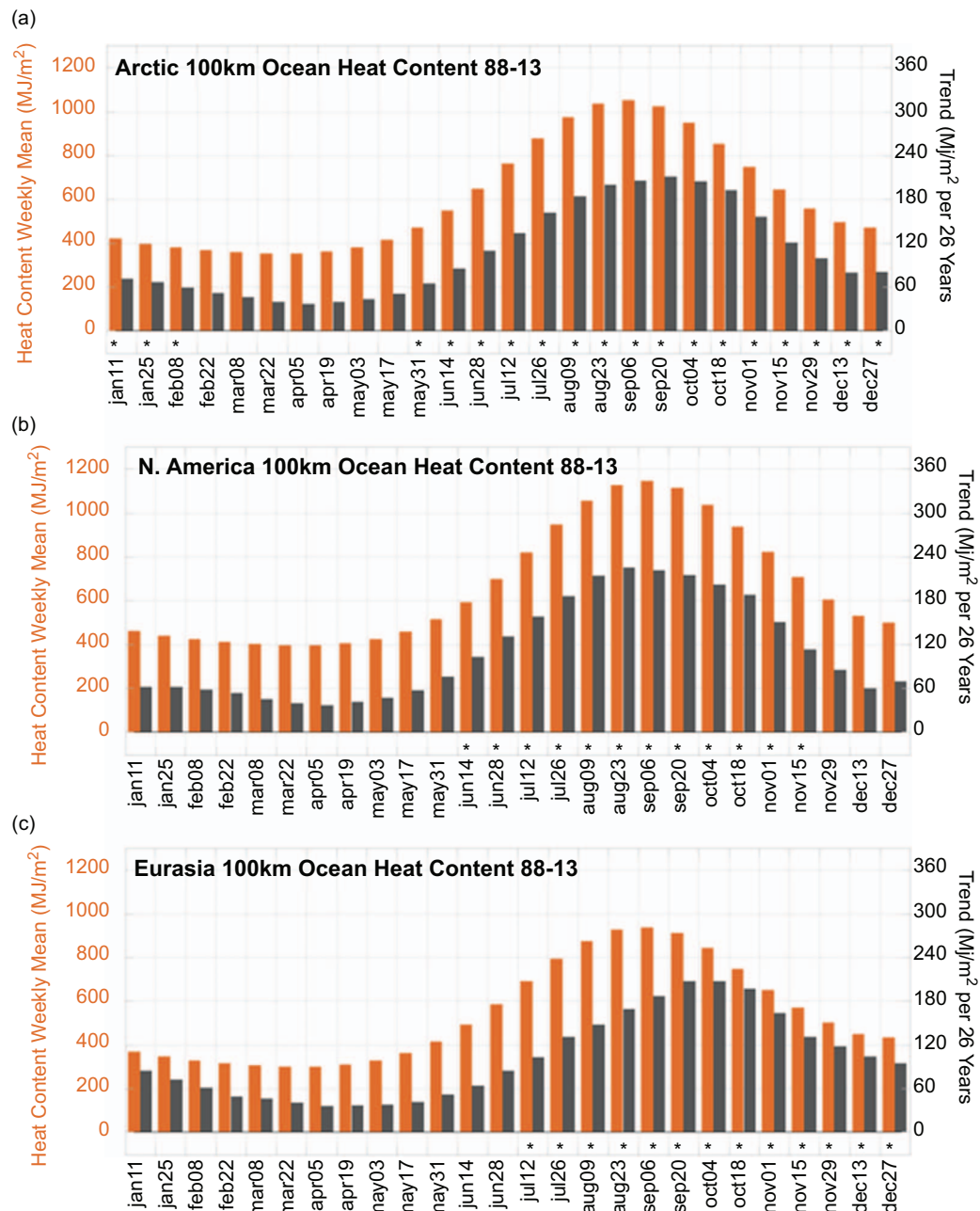


Figure 7. Arctic biweekly ocean heat content (orange bars) and trend (black bars) for 100 km zone from 1988–2013 for (a) Arctic, (b) North America, and (c) Eurasia. Biweekly trends statistically significant at the 95% level or greater are marked with an asterisk on the x-axis. Heat content is in units of MJ m^{-2} and trend is MJ m^{-2} over 26 years (1988–2013).

The 1982–2015 biweekly NDVI displays large positive trends during the peak of the growing season and weak negative trends in May and late September (figure 9(a)). Figure 9 displays biweekly NDVI climatology (green bars) and trends (grey bars) for the full period 1982–2015 (figure 9(a)), the early period of 1982–1998 (figure 9(b)) and the recent period from 1999–2015 (figure 9(c)). NDVI biweekly trends are strikingly different between the 1982–1998 and 1999–2015 period. During the 1982–1998 period (figure 9(b)), the NDVI increases were largest in spring indicating an earlier greenup, which is consistent with spring warming (figure 8(b)). NDVI trends for 1999–2015 show declines in the early and late parts of the growing season and positive trends during the

peak season (figure 9(c)). Spring temperatures trends are positive during the 1999–2015 period, so a lack of warmth cannot explain negative NDVI trends.

The initial story of sea ice decline leading to increased summer warmth and vegetation productivity (Bhatt *et al* 2010) now needs additional processes to explain the trends and variations evident in the recent data. The seasonality and time-series analysis indicate that since 1999 summer land surface temperatures have decreased in some parts of the Arctic, and biweekly spring NDVI has declined leading to declines since about 2001 in TI-NDVI. We next discuss how to understand the vegetation productivity trends in the context of ecological and climate drivers.

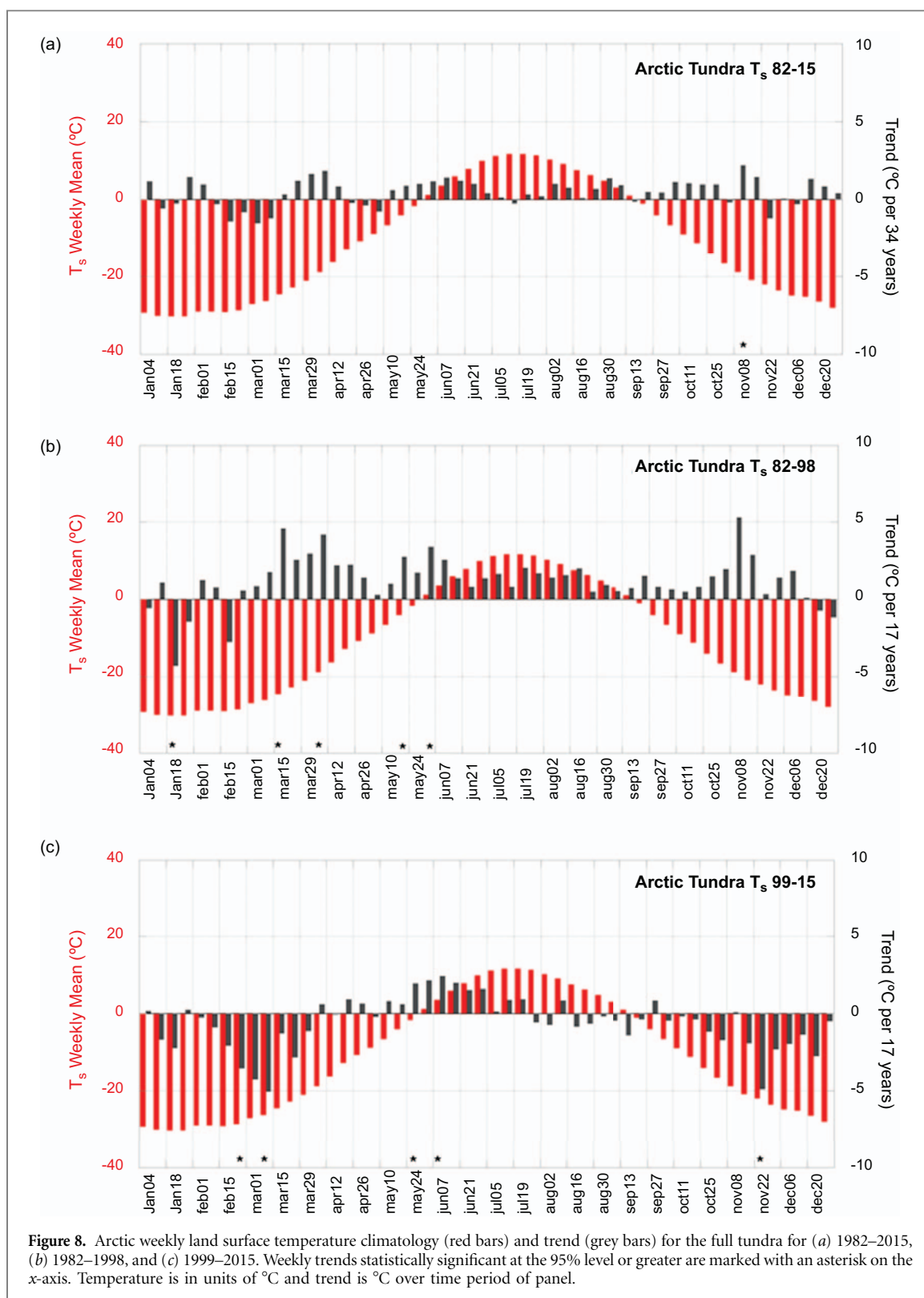


Figure 8. Arctic weekly land surface temperature climatology (red bars) and trend (grey bars) for the full tundra for (a) 1982–2015, (b) 1982–1998, and (c) 1999–2015. Weekly trends statistically significant at the 95% level or greater are marked with an asterisk on the x-axis. Temperature is in units of °C and trend is °C over time period of panel.

4. Discussion

4.1. Possible ecological drivers of the decline in spring-time NDVI

Panarctic trends of decreasing NDVI in May and June during 1999–2015 (figure 9(c)) represent the largest contribution to the TI-NDVI declines since 1999. This indicates that early-growing-season processes are likely causing the NDVI declines. Several

possibilities exist for the decline in springtime NDVI values.

4.1.1. Deeper, later-melting snowpack

The role of the timing of snow melt needs to be considered here because changes in the timing of snow melt strongly impact plant phenology (Zeng and Jia 2013) and especially the timing of greenup (Walker *et al* 1993 1999, Wahren *et al* 2005, Borner *et al* 2008,

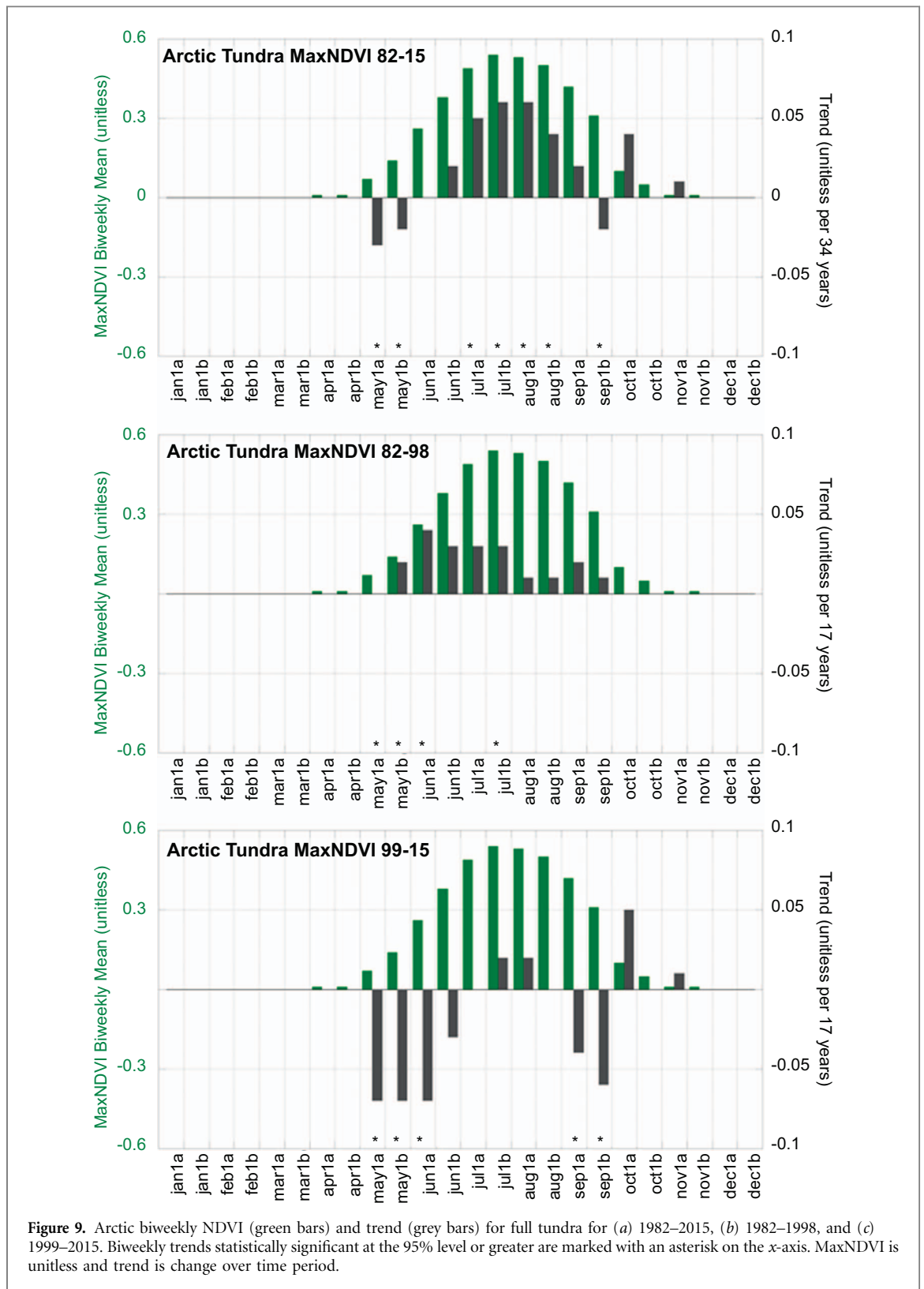


Figure 9. Arctic biweekly NDVI (green bars) and trend (grey bars) for full tundra for (a) 1982–2015, (b) 1982–1998, and (c) 1999–2015. Biweekly trends statistically significant at the 95% level or greater are marked with an asterisk on the x-axis. MaxNDVI is unitless and trend is change over time period.

Torp 2010, Callaghan *et al* 2012, Bienau *et al* 2014, Bjerke *et al* 2014, Bjorkman *et al* 2015). A logical cause of the observed decline in May–June NDVI would be that increased winter snowfall may be leading to later snow melt causing delayed phenology and decreased early-season NDVI (Walker *et al* 1993, Ellebjerg *et al* 2008). However, the June snow-cover extent (SCE) for the northern hemisphere has been declining at

increasingly rapid rates since 2005, and was –17% per decade for the period 1979–2015 (Derksen *et al* 2015). Thus, the springtime negative trend in NDVI is striking but not easily explained in light of reported sharply declining snow cover in North America and Eurasia in April, May, and June.

Bieniiek *et al* (2015) document increases in Alaska springtime snow-water equivalent based on the

GlobSnow reanalysis data (Takala *et al* 2011), which provides an inferred explanation for springtime MaxNDVI declines although the exact timing of snowmelt is not available in this data set. For this study we tried unsuccessfully to extend the GlobSnow conclusions for Alaska to the panarctic domain and since the results were fairly noisy they were not included. Long-term data sets able to identify the timing of snow melt specifically for the panarctic region are needed to test the hypothesis that snow is responsible for the declines in spring NDVI.

We suspect that major differences in the timing of melt are occurring in the warmer (early-melt) and colder (later-melt) parts of the Arctic, but we are aware of only one detailed analysis of station temperature, precipitation, and snow data along a coherent south-north transect in the Arctic. Vikhamar-Schuler *et al* (2010) investigated long-term climate data from four stations (Nadym, Salekhard, Tarko-Sale, and Mare-Sale) in the Yamalo-Nenets Autonomous Okrug, Russia. Reindeer herders, who migrate 1500 km between the Nadym region and Mare-Sale, are concerned about the increasing occurrence of severe weather, including rain-on-snow events that affect their reindeer's access to forage (Forbes *et al* 2016). The analysis showed major differences in the spring melt in the three southern stations (Nadym, Salekhard, Tarko-Sale) compared to the northernmost station at Mare-Sale. All the stations experienced warming from the periods 1961–1990 and 1979–2008 (overlapping 30 year period Salekhard experienced a 33% increase in precipitation between 1900 and 2008. Mare-Sale and Salekhard showed similar trends in snow cover between the 1930s up to the early 1980s. Then Salekhard experienced a considerable and persistent reduction in the snow season, mainly because of earlier melting in the spring, while the snow season at Mare-Sale after a short drop was prolonged. The reason for this difference is attributed by the authors to a combination of differences in the effect of the springtime temperature increase and differences in the precipitation patterns. This single example should not be used to infer similar circumpolar changes along south–north climate gradients, but it does suggest that more attention needs to be directed at the changes in the timing of spring snowmelt across the Arctic tundra climate gradient.

4.1.2. Increased water on the tundra

Recent studies have shown an increase in the amount of standing water in areas of ice-rich permafrost, throughout the Arctic, due to permafrost degradation (Liljedahl *et al* 2016, Jorgenson *et al* 2006, Farquharson *et al* 2016). Much of this water is in the form of small thermokarst ponds several meters to tens of meters in diameter, which are formed as the upper surface of the ice wedges melt and subside. For example, widespread and rapid thermokarst with extensive ponded freshwater occurred during the last

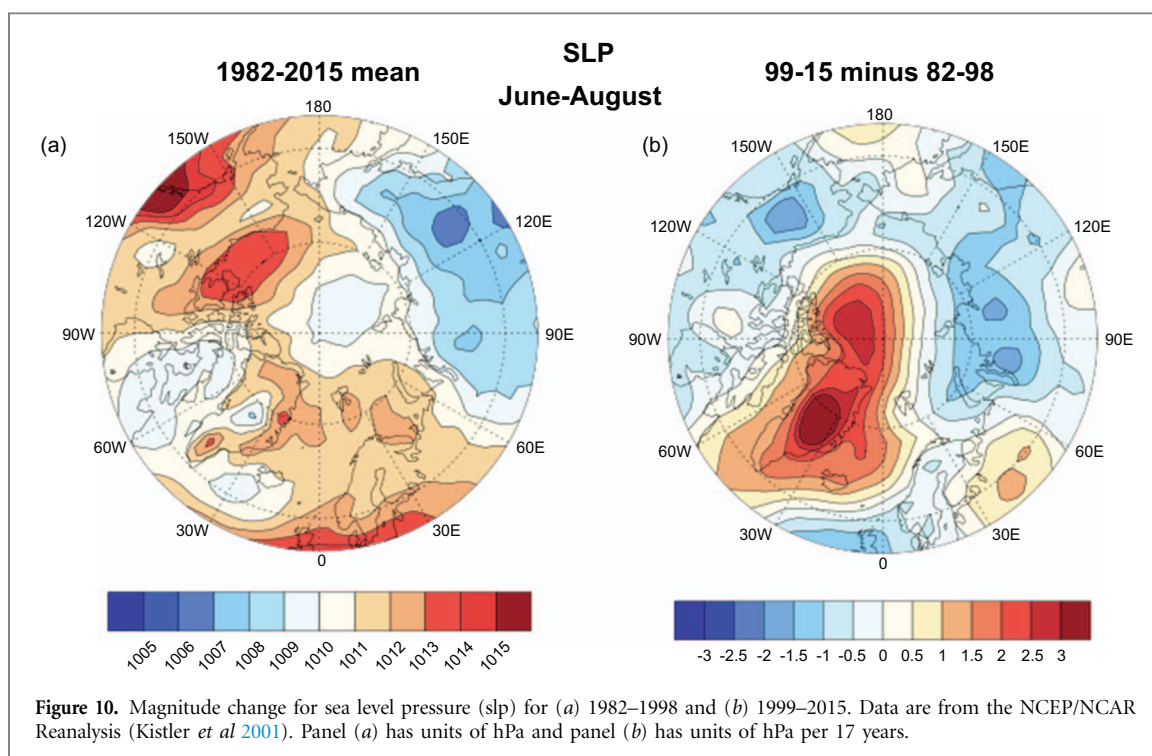
decade at High Arctic sites on Ellef Ringnes, Prince Patrick, and Banks Island, Canada. A warming summer climate caused warmer ground temperature, which increased active layer depth, ice-wedge melt, subsequent ground subsidence, and ponding (Farquharson *et al* 2016). NDVI is sensitive to soil moisture and water, both of which decrease NDVI values and can affect trends (Raynolds and Walker 2016). Any increases in snow will also cause an increase in meltwater in the early part of the growing season, as there is little opportunity for surface water to be absorbed in the ground because of shallow thaw. Standing water on the surface will contribute to a cooler land surface temperature but we currently have no evidence that this effect is stronger in Eurasia than North America, which is what we would expect to be consistent with the SWI trends shown in figure 4 (i.e. weak land surface temperature based SWI trends in Eurasia).

4.1.3. Killing frosts due to midwinter or early-spring snow melt

Other possible causes of decreasing spring NDVI include early season die-off of vegetation caused by mid-winter thaws exposing the tundra to extreme cold during winter (Bjerke *et al* 2014), hard frosts in spring after the tundra has become snow free (Inouye 2008) and midwinter rain-on-snow events (Forbes *et al* 2016). The combined contribution of multiple anomalous winter and spring weather events and outbreaks of moths contributed to a major decline in NDVI over a large area of maritime northern Norway in 2011–2012 in northern Norway (Bjerke *et al* 2014). We have also noted extensive browning events in northern Alaska in association with late frosts in 2015 and 2016, but these local events are difficult to invoke for the nearly circumpolar decline in TI-NDVI that we see since 1999.

4.1.4. Increased role of shrubs in spring browning

The shift in tundra vegetation from graminoid to deciduous shrubs may also contribute to the biweekly NDVI trends that are seen over the 1999–2015 period. Sweet *et al* (2014) documented a later budburst for tall deciduous vegetation compared to graminoid vegetation on the North Slope of Alaska because snow melt was delayed around the shrubs. In a subsequent study, Sweet *et al* (2015) found that shrubs extended the peak period without extending the growing season length. The continued increase during the peak with declines in spring of biweekly NDVI during 1999–2015 is consistent with increased deciduous shrub cover. This may be a valid explanation locally and regionally where shrub expansion has occurred, but it cannot explain the very widespread large-scale NDVI declines found in the GIMMS3g remote sensing record extending into the High Arctic where erect deciduous shrubs are absent.



4.2. Global climate drivers of Arctic trends

In addition to Arctic sea ice decline and changing cloud cover as climate drivers of tundra vegetation productivity, it is important to consider climate variations from lower latitudes, which transport moisture and heat poleward. For example, Ding *et al* (2014) analyzed annual mean climate observations and model data to argue that tropical forcing is responsible for the anomalous high over Greenland. Mean summer (June–August) sea-level pressure from the NCEP/NCAR Reanalysis is shown in figure 10(a) (update from figure 8(b) of Bhatt *et al* 2013) and is characterized by a high over the Beaufort Sea, low pressure over Eurasia and high pressure in North America. The sea-level-pressure (slp) difference pattern (1999–2015 minus 1982–1998) (figure 10(b)) displays a clear large-scale pattern showing that since 1999 slp has increased around Greenland and decreased over Eurasia and western North America. During summer, lower slp typically indicates increased cloudiness and cooling while higher slp indicates clearer skies and warming. These recent decreases of slp over the tundra region are consistent with generally lower SWI values. This suggests that the large-scale circulation likely contributes to the recent decline of summer warmth over most of the Arctic tundra.

As the global climate has warmed and the hydrological cycle has intensified (Huntington and Billmire 2014), atmospheric moisture (Del Genio *et al* 1991) and poleward moisture transport have increased (Held and Soden 2006). How the increased global hydrological cycle is manifest in the Arctic is not well documented particularly during the growing season but Zhang *et al* (2012) have shown that winter time moisture transport into Eurasia has increased.

Moisture effects on tundra vegetation productivity are receiving increased research efforts. Delidjakova *et al* (2016) found that increased onshore winds from Hudson Bay advected cool moist air over the tundra and resulted in increased vegetation productivity. Where climatological moisture levels are higher, such as in Western Eurasia compared to North America, biomass, particularly moss biomass, is larger in the moisture-rich areas for the same bioclimate subzone (Walker *et al* 2012b). Most of the atmospheric moisture available for precipitation in the Arctic is transported from lower latitudes, but a recent analysis of precipitation deuterium excess data documents an increase of moisture originating from the Arctic (Kopeck *et al* 2016). Consistent with the idea of increased moisture from Arctic sources, cloud cover over the Arctic Ocean has increased as sea ice has decreased (Liu *et al* 2012). There is also evidence that precipitation has increased over the Arctic during the warm season. Kokelj *et al* (2015) conclude that the recent increase in the number and size of active thaw slumps over the Mackenzie basin is linked to precipitation increases. Changes in moisture transport from lower latitudes and increased local moisture need to be investigated further to understand recent vegetation productivity declines to better anticipate future biomass changes in the Arctic tundra.

5. Summary and conclusions

This study employs remote sensing data in the Arctic to explore the seasonality and update recent trends of sea ice and oceanic heat content in the coastal oceans and land surface temperatures, maximum NDVI and

time-integrated NDVI over the tundra. The summary for the panarctic tundra is as follows. During the 1982–2015 period, summer sea ice declined while oceanic heat content increased. Summer warmth index (SWI) increased until mid-1990s and remained flat until the last two years when it began to increase again. MaxNDVI increased over the full period while TI-NDVI declined since the early 2000s. Comparing trends for 1982–1998 to 1999–2015 reveals that negative trends were more common during the latter period for MaxNDVI and TI-NDVI.

The climatology and trends of the weekly sea ice, biweekly ocean-heat content, weekly land surface temperature and biweekly NDVI were calculated to investigate the seasonality of changes in the panarctic. Sea ice decline was larger during spring during the 1982–1998 period compared to 1999–2015, while fall sea ice decline was larger in the later period. Oceanic heat content is at its climatological maximum in early September for the panarctic and the largest positive trends occurred within a few weeks of this maximum. Land surface temperatures are above zero Celsius from late May to late August and displayed positive trends most of the year during the 1982–1998 period and displayed negative trends most of the year except late spring to early summer during 1999–2015. The biweekly NDVI reached its climatological peak in the second half of July and during the 1982–1998 period the largest positive trends occur in spring, consistent with increased vegetation productivity early in the season. Biweekly NDVI trends from 1999–2015 displayed significant negative trends in May and the first half of June, suggesting that there are processes delaying green-up. There were also significant negative trends in September during the 1999–2015 period for the panarctic biweekly NDVI.

Our current understanding does not allow us to identify the drivers responsible for the recent declines in vegetation productivity. As sea ice decline has continued, other processes such as increased cloudiness may be coming into play and reducing summer temperatures. However, the early growing season declines in NDVI coincide with warming temperatures, not cooling, so require an alternate explanation. Numerous possible climate and ecological drivers of NDVI decline from across the panarctic tundra have been discussed in the manuscript: increased standing water, delayed spring snow-melt, winter thaw events, increased shrub cover, and early snow melt followed by freezing temperatures. Each of these pathways has been documented over fairly localized areas so cannot explain the large scale of the spatial TI-NDVI trends. Since most models predict Arctic greening, it is vital to understand the drivers of the recent browning (Phoenix and Bjerke 2016). A synthesis study that jointly considers vegetation type, permafrost conditions, elevation, as well as climate factors such as temperature, heat and moisture transport, and timing of snowfall and spring snowmelt is needed to better

understand recent tundra vegetation productivity declines.

Acknowledgments

This work benefitted from fruitful conversations with Ross Brown, Chris Derksen, David Robinson, Walt Meier, Gus Shaver, and Stein Rune Karlsen. This study was supported by NASA/NEESPI Land Cover Land Use Change Initiative, Grant No. NNG6GE00A, NNX09AK56G and NNX14AD90G; National Science Foundation grants ARC-0902175 and ARC-1203506; and NASA NNH16CP09C–Arctic Boreal Vulnerability Experiment.

References

- Alexeev V A, Langen P L and Bates J R 2005 Polar amplification of surface warming on an aquaplanet in 'ghost forcing' experiments without sea ice feedbacks *Clim. Dynam.* **24** 655–66
- Bekryaev R V, Polyakov I V and Alexeev V A 2010 Role of polar amplification in long-term surface air temperature variations and modern Arctic warming *J. Clim.* **23** 3888–906
- Bhatt U S, Walker D A, Raynolds M K, Bieniek P A, Epstein H E, Comiso J C, Pinzon J E, Tucker C J and Polyakov I V 2013 Recent declines in warming and vegetation greening trends over Pan-Arctic tundra *Remote Sens.* **5** 4229–54
- Bhatt U S *et al* 2010 Circumpolar Arctic tundra vegetation change is linked to sea ice decline *Earth Interact.* **14** 1–20
- Bienau M J, Hattermann D, Kröncke M, Kretz L, Otte A, Eiserhardt W L, Milbau A, Graae B J, Durka W and Eckstein R L 2014 Snow cover consistently affects growth and reproduction of *Empetrum hermaphroditum* across latitudinal and local climatic gradients *Alp. Bot.* **124** 115–29
- Bieniek P A *et al* 2015 Climate drivers linked to changing seasonality of Alaska coastal tundra vegetation productivity *Earth Interact.* **19** 1–29
- Bjerke J W, Rune Karlsen S, Arild Høgda K, Malnes E, Jepsen J U, Lovibond S, Vikhamar-Schuler D and Tømmervik H 2014 Record-low primary productivity and high plant damage in the Nordic Arctic region in 2012 caused by multiple weather events and pest outbreaks *Environ. Res. Lett.* **9** 084006
- Bjorkman A D, Elmendorf S C, Beamish A L, Vellend M and Henry G H R 2015 Contrasting effects of warming and increased snowfall on Arctic tundra plant phenology over the past two decades *Glob. Change Biol.* **21** 4651–61
- Bliss L C 1997 Arctic ecosystems of North America *Polar and Alpine Tundra* (Amsterdam: Elsevier) pp 551–683
- Borner A P, Kielland K and Walker M D 2008 Effects of simulated climate change on plant phenology and nitrogen mineralization in Alaskan Arctic tundra *Arctic* **40** 27–38
- Bulygina O N, Razuvaev V N and Korshunova N N 2009 Changes in snow cover over Northern Eurasia in the last few decades *Environ. Res. Lett.* **4** 045026
- Callaghan T V *et al* 2012 Multiple effects of changes in Arctic snow cover *Ambio* **40** 32–45
- Callaghan T V *et al* 2004 Biodiversity, distributions and adaptations of Arctic species in the context of environmental change *Ambio* **33** 404–17
- Chernov Y I and Matveyeva N V 1997 Arctic ecosystems in Russia *Polar and Alpine Tundra* ed F E Wielgolaski (Amsterdam: Elsevier) pp 361–507

- Cherry J, Déry S, Cheng Y, Stieglitz M, Jacobs M and Pan F 2014 Climate and hydrometeorology of the Toolik Lake Region and the Kuparuk River Basin: past, present and future *Alaska's Changing Arctic: Ecological Consequences for Tundra, Streams and Lakes* (New York: Oxford University Press) pp 310
- Clow G D 2014 Temperature data acquired from the DOI/GTN-P deep borehole array on the Arctic slope of Alaska, 1973–2013 *Earth Sys. Sci. Data* **6** 201–18
- Cohen J L, Furtado J C, Barlow M A, Alexeev V A and Cherry J E 2012 Arctic warming, increasing snow cover and widespread boreal winter cooling *Environ. Res. Lett.* **7** 014007
- Comiso J C 2003 Warming trends in the Arctic from clear sky satellite observations *J. Clim.* **16** 3498–510
- Comiso J C and Nishio F 2008 Trends in the sea ice cover using enhanced and compatible AMSR-E, SSM/I, and SMMR data *J. Geophys. Res.* **113** C02S07
- Dee D P *et al* 2011 The ERA-interim reanalysis: configuration and performance of the data assimilation system *Q. J. R. Meteor. Soc.* **137** 553–97
- Del Genio A D, Laci A A and Ruedy R A 1991 Simulations of the effect of a warmer climate on atmospheric humidity *Nature* **351** 382–5
- Delidjakova K K, Bello R L and Higuchi K 2016 Influence of Hudson Bay on the carbon dynamics of a Hudson Bay lowlands coastal site *Arctic Sci.* **2** 142–63
- Derksen C, Brown R, Mudryk L and Luojus K 2015 Terrestrial snow cover snow *Arctic Report Card 2015* ed M O Jeffries J Richter-Menge J E Overland (Silver Spring, MD: NOAA)
- Ding Q, Wallace J M, Battisti D S, Steig E J, Gallant A J E, Kim H-J and Geng L 2014 Tropical forcing of the recent rapid arctic warming in northeastern Canada and Greenland *Nature* **509** 209–12
- Dutrieux L P, Bartholomeus H, Herold M and Verbesselt J 2012 Relationships between declining summer sea ice, increasing temperatures and changing vegetation in the Siberian Arctic tundra from MODIS time series 2000–11 *Environ. Res. Lett.* **7** 044028
- Easterling D R and Wehner M F 2009 Is the climate warming or cooling? *Geophys. Res. Lett.* **36** L08706
- Ellebjerg S M, Tamstorf M P, Illeris L, Michelsen A and Hansen B U 2008 Inter-annual variability and controls of plant phenology and productivity at Zackenberg *High-Arctic Ecosystem Dynamics in a Changing Climate (Advances in Ecological Research)* vol 40 (Amsterdam: Elsevier) pp 249–73 ([https://doi.org/10.1016/S0065-2504\(07\)00011-6](https://doi.org/10.1016/S0065-2504(07)00011-6))
- Epstein H E, Bhatt U S, Reynolds M K, Walker D A, Forbes B C, Macias-Fauria M, Lorant M, Phoenix G and Bjerke J 2016 Tundra greenness *Arctic Report Card 2016* ed M O Jeffries, J Richter-Menge and J E Overland (Silver Spring, MD: NOAA)
- Epstein H *et al* 2015 Tundra greenness *Arctic Report Card 2015* ed M O Jeffries, J Richter-Menge and J E Overland (Silver Spring, MD: NOAA)
- Epstein H E, Reynolds M K, Walker D A, Bhatt U S, Tucker C J and Pinzon J E 2012 Dynamics of aboveground phytomass of the circumpolar Arctic tundra during the past three decades *Environ. Res. Lett.* **7** 015506
- Farquharson L M, Romanovsky V E, Cable W L and Walker D A 2016 Widespread and rapid thermokarst development in a region of very cold continuous permafrost in the Canadian High Arctic *AGU Fall Meeting (San Francisco, CA 12–16 December)*
- Forbes B C *et al* 2016 Sea ice, rain-on-snow and tundra reindeer nomadism in Arctic Russia *Biol. Lett.* **12** 20160466–5
- Held I M and Soden B J 2006 Robust responses of the hydrological cycle to global warming *J. Clim.* **19** 5686–99
- Hope A, Engstrom R and Stow D 2005 Relationship between AVHRR surface temperature and NDVI in Arctic tundra ecosystems *Int. J. Remote Sens.* **26** 1771–6
- Huntington T G and Billmire M 2014 Trends in precipitation, runoff, and evapotranspiration for rivers draining to the Gulf of Maine in the United States *J. Hydrometeorol.* **15** 726–43
- Inouye D W 2008 Effects of climate change on phenology, frost damage, and floral abundance of mountain wildflowers *Ecology* **89** 353–62
- Jia G J, Epstein H E and Walker D A 2003 Greening of Arctic Alaska, 1981–2001 *Geophys. Res. Lett.* **30** 2067
- Jorgenson M T, Shur Y L and Pullman E R 2006 Abrupt increase in permafrost degradation in Arctic Alaska *Geophys. Res. Lett.* **33** L02503
- Ju J and Masek J G 2016 The vegetation greenness trend in Canada and US Alaska from 1984–2012 Landsat data *Remote Sens. Environ.* **176** 1–16
- Kapnick S B and Delworth T L 2013 Controls of global snow under a changed climate *J. Clim.* **26** 5537–62
- Kistler R *et al* 2001 The NCEP-NCAR 50 year reanalysis: monthly means CD-ROM and documentation *Bull. Amer. Meteorol. Soc.* **82** 247–68
- Kohler J, Brandt O, Johansson M and Callaghan T 2006 A long-term Arctic snow depth record from Abisko, northern Sweden, 1913–2004 *Polar Res.* **25** 91–113
- Kokelj S V, Tunnicliffe J, Lacle D, Lantz T C, Chin K S and Fraser R 2015 Increased precipitation drives mega slump development and destabilization of ice-rich permafrost terrain, northwestern Canada *Glob. Planet. Change* **129** 56–68
- Kopec B G, Feng X, Michel F A and Posmentier E S 2016 Influence of sea ice on Arctic precipitation *Proc. Natl Acad. Sci.* **113** 46–51
- Krasting J P, Broccoli A J, Dixon K W and Lanzante J R 2013 Future changes in northern hemisphere snowfall *J. Clim.* **26** 7813–28
- Liljedahl A K *et al* 2016 Pan-arctic ice-wedge degradation in warming permafrost and its influence on tundra hydrology *Nat. Geosci.* **9** 312–8
- Liu Y, Key J R, Liu Z, Wang X and Vavrus S J 2012 A cloudier Arctic expected with diminishing sea ice *Geophys. Res. Lett.* **39** L05705
- Mudelsee M 2009 Break function regression *Eur. Phys. J. Spec. Top.* **174** 49–63
- Mudelsee M 2010 *Climate Time Series Analysis* vol 42 (Dordrecht: Springer)
- Myneni R B, Keeling C D, Tucker C J, Asrar G and Menani R R 1997 Increased plant growth in the northern high latitudes from 1981 to 1991 *Nature* **386** 698–702
- Phoenix G K and Bjerke J W 2016 Arctic browning: extreme events and trends reversing arctic greening *Glob. Change Biol.* **22** 2960–2
- Pinzon J and Tucker C 2014 A non-stationary 1981–2012 AVHRR NDVI3g time series *Remote Sens.* **6** 6929–60
- Polyakov I V, Bhatt U S and Walsh J E 2013 Recent oceanic changes in the Arctic in the context of longer term observations *Ecol. Appl.* **23** 1745–64
- Reynolds M K and Walker D A 2016 Increased wetness confounds landsat-derived NDVI trends in the central Alaska North Slope region, 1985–2011 *Environ. Res. Lett.* **11** 085004
- Reynolds M K, Walker D A, Munger C A, Vonlanthen C M and Kade A N 2008 A map analysis of patterned-ground along a North American Arctic Transect *J. Geophys. Res.* **113** G03S03
- Roberts C D, Palmer M D, McNeill D and Collins M 2015 Quantifying the likelihood of a continued hiatus in global warming *Nat. Clim. Change* **5** 337–42
- Santer B D, Wigley T M L, Boyle J S, Gaffen D J, Hnilo J J, Nychka D, Parker D E and Taylor K E 2000 Statistical significance of trends and trend differences in layer-average atmospheric temperature time series *J. Geophys. Res.* **105** 7337–56
- Screen J A and Simmonds I 2010 The central role of diminishing sea ice in recent Arctic temperature amplification *Nature* **464** 1334–7
- Shiklomanov N I and Streletskiy D 2015 Circumpolar Active Layer Monitoring (CALM) program: long-term monitoring of the active layer/upper permafrost system *Arctic Observing Open Science Meeting (Fairbanks, Alaska)* (www.arcus.org/search-program/meetings/2015/aossm/presentations)

- Shippert M M, Walker D A, Auerbach N A and Lewis B E 1995 Biomass and leaf-area index maps derived from SPOT images for Toolik Lake and Imnavait Creek areas *Alaska Polar Record* **31** 147–54
- Steele M, Ermold W and Zhang J 2011 Modeling the formation and fate of the near-surface temperature maximum in the Canadian Basin of the Arctic Ocean *J. Geophys. Res.* **116** C11015
- Stow D A *et al* 2004 Remote sensing of vegetation and land-cover change in Arctic Tundra ecosystems *Remote Sens. Environ.* **89** 281–308
- Sweet S K, Griffin K L, Steltzer H, Gough L and Boelman N T 2015 Greater deciduous shrub abundance extends tundra peak season and increases modeled net CO₂ uptake *Glob. Change Biol.* **21** 2394–409
- Sweet S K, Gough L, Griffin K L and Boelman N T 2014 Tall deciduous shrubs offset delayed start of growing season through rapid leaf development in the Alaskan Arctic tundra *Arct. Antarct. Alp. Res.* **46** 682–97
- Takala M, Luojus K, Pulliainen J, Derksen C, Lemmetyinen J, Kärnä J-P, Koskinen J and Bojkov B 2011 Estimating Northern Hemisphere snow water equivalent for climate research through assimilation of space-borne radiometer data and ground-based measurements *Remote Sens. Environ.* **115** 3517–29
- Torp M 2010 The Effect of Snow on Plants and Their Interactions with Herbivores *PhD Thesis* University of Umea, Sweden 59 pp
- Tucker J and Sellers P J 1986 Satellite remote sensing of primary production *Int. J. Rem. Sens.* **7** 1395–416
- Urban M, Eberle J, Huttich C, Schmuilius V and Herold M 2013 Comparison of satellite-derived land surface temperature and air temperature from meteorological stations on the pan-Arctic scale *Remote Sens.* **5** 2348–67
- Urban F E and Clow G D 2014 DOI/GTN-P climate and active-layer data acquired in the National Petroleum Reserve-Alaska and the Arctic National Wildlife Refuge *Data Series 892 report* (Reston, VA: USGS) (<https://doi.org/10.3133/ds892>)
- Vikhamar-Schuler D, Hanssen-Bauer I and Førland E J 2010 Long-term climate trends of the Yamalo-Nenets AO, Russia *Norwegian Meteorological Institute Report* 51 pp
- Wahren C H A, Walker M D and Bret-Harte M S 2005 Vegetation responses in Alaskan Arctic tundra after 8 years of a summer warming winter snow manipulation experiment *Glob. Change Biol.* **11** 537–52
- Walker D A, Bhatt U S, Epstein H E, Bieniek P, Comiso J, Frost G V, Pinzon J, Reynolds M K and Tucker C J 2012a Changing Arctic tundra vegetation biomass and greenness *Bull. Am. Meteorol. Soc.* **93** S138–9
- Walker D A *et al* 2012b Environment, vegetation and greenness (NDVI) along the North America and Eurasia Arctic transects *Environ. Res. Lett.* **7** 015504
- Walker D A *et al* 2009 Arctic: land: vegetation 'state of the climate in 2009' *Bull. Am. Meteorol. Soc.* **91** S79–82
- Walker D A *et al* 2005 The circumpolar Arctic vegetation map *J. Veg. Sci.* **16** 267–82
- Walker D A, Epstein H E, Jia G J, Balsler A, Copass C, Edwards E J, Gould W A, Hollingsworth J, Knudson J and Maier H A 2003a Phytomass, LAI, and NDVI in northern Alaska: relationships to summer warmth, soil pH, plant functional types, and extrapolation to the circumpolar Arctic *J. Geophys. Res.* **108** 8169
- Walker D A *et al* 2003b Vegetation-soil-thaw-depth relationships along a low-arctic bioclimate gradient, Alaska: synthesis of information from the ATLAS studies *Permafrost Periglacial Process.* **14** 103–23
- Walker D A, Halfpenny J C, Walker M D and Wessman C 1993 Long-term studies of snow-vegetation interactions *BioScience* **43** 287–301
- Walker M D *et al* 1999 Long-term experimental manipulation of winter snow regime and summer temperature in Arctic and alpine tundra *Hydrol. Process.* **13** 2315–30
- Xu L *et al* 2013 Temperature and vegetation seasonality diminishment over northern lands *Nat. Clim. Change* **3** 581–6
- Zeng H and Jia G 2013 Impacts of snow cover on vegetation phenology in the Arctic from satellite data *Adv. Atmos. Sci.* **30** 1421–32
- Zhang X, He J, Zhang J, Polyakov I, Gerdes R, Inoue J and Wu P 2012 Enhanced poleward moisture transport and amplified northern high-latitude wetting trend *Nat. Clim. Change* **3** 47–51
- Zhang J and Rothrock D A 2003 Modeling global sea ice with a thickness and enthalpy distribution model in generalized curvilinear coordinates *Mon. Weath. Rev.* **131** 681–97